Optimizing thin film solar voltaic components

Peter Monk

University of Delaware, USA

Research support in part by an NSF-SOLAR grant

Outline

This talk will be about designing multiplasmonic solar cells and solar concentrators, and beam splitters:

- Introduction to the project and plasmonics
- Design Problems
- Validation for the solar cell
- Numerical analysis
- Optimizing the beam splitter
- The time domain

Surface Plasmons

Suppose we have an interface[1] between two materials at $z = 0$ with electromagnetic parameters μ_0 and ϵ_i, $i = 1, 2$ respectively.

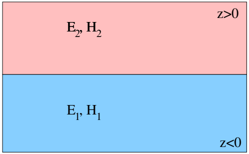

$$\nabla \times \boldsymbol{H}_i = \epsilon_i \frac{1}{c} \frac{\partial \boldsymbol{E}_i}{\partial t}$$
$$\nabla \times \boldsymbol{E}_i = -\frac{1}{c} \frac{\partial \boldsymbol{H}_i}{\partial t}$$

Assuming p-polarization, we seek solutions localized at the boundary $z = 0$,

$$\boldsymbol{E}_i = (E_x^i, 0, E_z^i)\mathrm{e}^{-\kappa_i|z|}\mathrm{e}^{\mathrm{i}(qx-\omega t)} \text{ and } \boldsymbol{H}_i = (0, H_y^i, 0)\mathrm{e}^{-\kappa_i|z|}\mathrm{e}^{\mathrm{i}(qx-\omega t)}$$

To satisfy Maxwell:

$$\kappa_i = \sqrt{q^2 - \epsilon_i \omega^2 / c^2}.$$

[1] This introduction is taken from J. Pitarke et al, *Rep. Prog. Phys.*, **70** (2007) 1-87

Plasmon condition

Continuity at $z = 0$ of tangential components requires,

$$\frac{\epsilon_1}{\kappa_1} + \frac{\epsilon_2}{\kappa_2} = 0$$

Suppose $\epsilon_2 = 1$ and the metal is described by a Drude model:

$$\epsilon_2 = 1 - \frac{\omega_p^2}{\omega(\omega + \mathrm{i}\eta)}$$

The plot shows ω versus $\Re(q)$ when $\eta = 0$. Red line: $\omega_s = \omega_p/\sqrt{2}$, Green line: $\omega = cq$. Note $\Re(\epsilon_2) < 0$ for ω small enough.

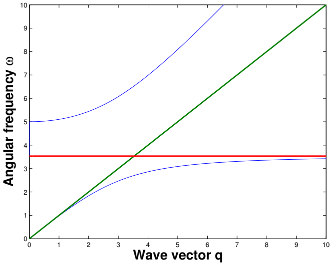

SPPs in photovoltaics[2]

- Motivation:

  To absorb light well, Silicon solar cells need to be thick. But efficiency (and cost!) motivate thin film cells.

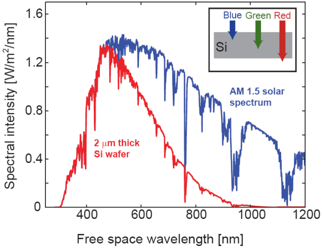

- If incident light couples into SPP modes, these modes might trap and guide light allowing a thinner or more efficient cell.

[2] From: H. Atwater and A. Polman, *Nature Materials*, **9** (2010) 205-213

SPPs in photovoltaics

A problem:

Incident light will not couple to SPP waves in a planar structure.

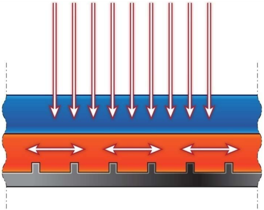

A metal grating can be used to generate surface waves.

SOLAR project

Our project[3] started with the work of M. Faryad and A. Lakhtakia [4] showing that if ϵ_1 is periodic in z multiple SPP modes exist at each frequency.

Penn State		Delaware	
T. Mallouk (PI)	Chemistry	Monk	Math
T. Mayer	Electrical Engineering	M. Solano	Math
A. Lakhtakia	Eng. Science and Mech,	L. Fan	Math
G. Barber	Chemistry		
M. Faryad	Eng. Science and Mech.		
L. Liu	Eng. Science and Mech.		
S. Hall	Chemistry		

[3] NSF-DMR-1125591

[4] See for example, M. Faryad and A. Lakhtakia, J. Opt. Soc. Am. B. **27** (2010) 2218-2223

Typical Structures

Wavelength of light of interest: 400-1200nm
Period of the grating: $\approx$ 400nm
Height of structure: $\approx$ 2000nm

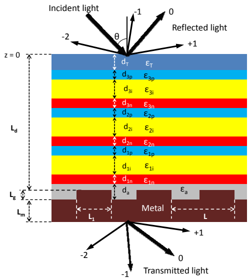

Thin film solar cell[5].

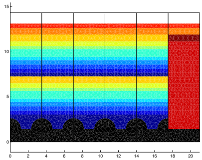

Concentrator. [6]

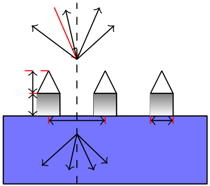

Beam splitter[7]

[5] M. Solano et al, Applied Optics, **52** (2013) 966-979
[6] M. Solano et al., Appl. Phys. Lett. **103**, 191115, 2013
[7] L. Fan et al., SPIE San Diego, 2014

Basic Multi-SPP cell

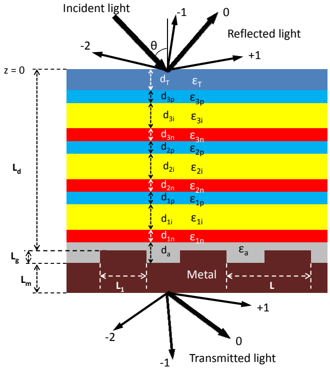

Incident field: Let $k = \omega/c$
$u^i = \exp(\mathrm{i}k(x \sin\theta + z\cos\theta))$.
Equations:

$$\begin{aligned} \nabla \cdot A\nabla u + k^2 nu &= 0 \text{ in } (0, L) \times \mathbb{R} \\ \mathrm{e}^{-\mathrm{i}kL\sin\theta} u(x + L, z) &= u(x, z) \text{ for all } x, z \\ u^i + u^s &= u \text{ in } (0, L) \times \mathbb{R}. \end{aligned}$$

and u^s satisfies upward and downward propagating wave conditions above and below the cell.

For s polarization: $A = 1$, $n = \epsilon_r$, $u = E_2$
For p-polarization: $A = 1/\epsilon_r$, $n = 1$, $u = H_2$.

Above and below the grating

For $z < 0$:

$$u^s = \sum_{n \in \mathbb{Z}} u_n^s \exp\left[i\left(k_x^{(n)} x - k_z^{(n)} z\right)\right],$$

where $k_x^{(n)} = k \sin\theta + 2\pi n/L$,

$$k_z^{(n)} = \begin{cases} \sqrt{k^2 - \left(k_x^{(n)}\right)^2}, & k^2 > \left(k_x^{(n)}\right)^2 \\ i\sqrt{\left(k_x^{(n)}\right)^2 - k^2}, & k^2 < \left(k_x^{(n)}\right)^2 \end{cases},$$

Similarly for the transmitted wave in $z > 0$ and $|z|$ large enough.

$$u^t = \sum_{n \in \mathbb{Z}} u_n^t \exp\left[i\left(k_x^{(n)} x + k_z^{(n)} z\right)\right],$$

Computed Quantities

For s-polarized incidence, we compute the modal reflectances

$$R_s^{(n)} = |u_n^s|^2 \,\mathrm{Re}\left[k_z^{(n)}\right]/(k\cos\theta)$$

and modal transmittances

$$T_s^{(n)} = |u_n^t|^2 \,\mathrm{Re}\left[k_z^{(n)}\right]/(k\cos\theta)\,.$$

The *absorptance* for s-polarized incident waves is given by

$$A_s = 1 - \sum_{n=-N_t}^{N_t}\left[R_s^{(n)} + T_s^{(n)}\right].$$

Similar definitions hold for p-polarized waves.

Variational Formulation

Let $\Omega = (0, L) \times (0, H)$ where H is the height of the cell

$$H^1_{qp}(\Omega) = \{u \in H^1(\Omega) \mid u(L, \cdot) = \exp(\mathrm{i}kL\sin\theta)u(0, \cdot)\}$$

Seek $u \in H^1_{qp}(\Omega)$ such that

$$\int_\Omega A\nabla u \cdot \nabla \overline{v} - k^2 n u \overline{v} - \int_{\Gamma_H} T_H u \overline{v} + \int_{\Gamma_0} (T_0(u - u^i) + u^i)\overline{v} = 0$$

for all $v \in H^1_{qp}(\Omega)$ where T_H is the Dirichlet to Neumann map on the upper surface Γ_H and similarly T_0 on Γ_0. These are computed using the Fourier representation of the solution above and below the grating.

Numerical Method (I): Finite Element Methods

Let

$$S_h \subset H^1_{qp}(\Omega)$$

Seek $u_{h,N} \in S_h$ such that

$$\int_\Omega A\nabla u_{h,N} \cdot \nabla \overline{v} - k^2 n u_{h,N} \overline{v}\, dA \\ - \int_{\Gamma_H} T_H P_N u_{h,N} \overline{v}\, ds + \int_{\Gamma_0} (T_0 P_N (u_{h,N} - u^i) + u^i) \overline{v}\, ds = 0$$

for all $v \in S_h$ where P_N is L^2 projection onto the space spanned by Fourier basis functions of degree n, $-N \leq n \leq N$.

Note: this requires the mesh on the left and right edges to be identical.

Theoretical papers

- Uniqueness problems: Uniqueness except at a countable set of exceptional frequencies [8]
- Grating theory and numerical analysis.[9]
- Goal oriented adaptivity.[10].

---

[8] A.S. Bonnet-Bendhia and F. Starling, Mathematical Methods in the Applied Sciences, **17** (1994), 305-338.

[9] A. Kirsch: Diffraction by periodic structures, *Inverse Problems in Mathematical Physics* (1993), L. Paivarinta and E. Somersalo, Eds., pp. 87–102, A. Kirsch and P. Monk, IMA J. Numer. Anal., **10**(1990) 425-447, G.C. Hsiao, N. Nigam and J. Pasciak, J. Comp. Appl. Math. **235**(2011) 4949-4965, J. Elschner and G.Schmidt, Math. Meth. Appl. Sci., **21**(1998), 1297-1342 (1998)

[10] N.H.Lord and A.J. Mulholland, Proc. Roy. Soc. 469(2013), 20130176

Numerical Method (II): Rigorous Coupled Wave Expansion (RCWA)

RCWA[11] is a commonly used scheme for this type of problem. The relative permittivity in the region $0 \leq z \leq H$ is expanded as a Fourier series with respect to x:

$$\epsilon(x,z) = \sum_{n \in \mathbb{Z}} \epsilon^{(n)}(z) \exp(i2\pi nx/L) , \qquad z \in [0,H] \ ,$$

where the z-dependent coefficients $\epsilon^{(n)}(z)$ are known. The electric field is similarly expanded

$$u(x,z) = \sum_{n \in \mathbb{Z}} u^{(n)}(z) \exp\left(i2\pi nx/L\right) \ , \ z \in [0,H] \, .$$

[11] L. Li, J. Opt. Soc. Am. A 12, 2581 (1993).

Discretization in z

- The Fourier series are substituted into the Maxwell system and the results truncated to order N
- The grating is divided into horizontal layers, and $\epsilon^{(n)}(z)$ is approximated by its mid-layer value.
- The resulting coupled system of ordinary differential equations in z is solved exactly and the map between incident, transmitted and reflected fields can be computed.
- The layers are combined by marching using a splitting into upward and downward going waves to help stabilize the procedure.

Basic Multi-SPP cell

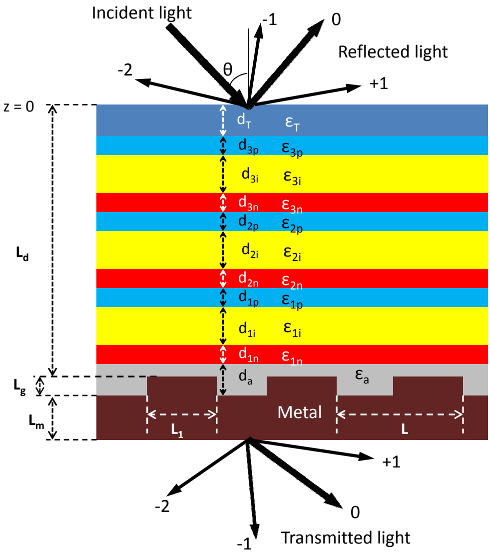

Frequency dependence of coefficients

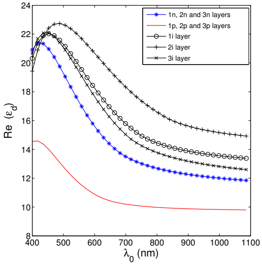

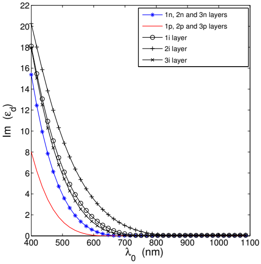

(Left) Real and (right) imaginary parts of the relative permittivities of all semiconductor layers as functions of the free-space wavelength.

Relative permittivity of aluminum

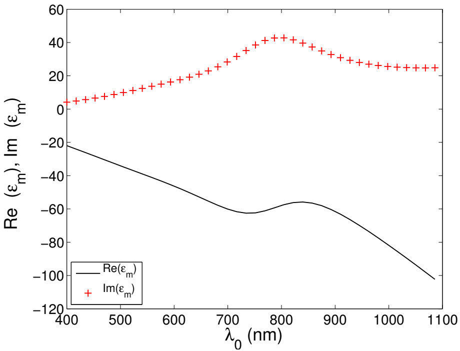

Real and imaginary parts of the relative permittivity of aluminum as functions of the free-space wavelength.

Grating profiles I

Experimental setup[12]

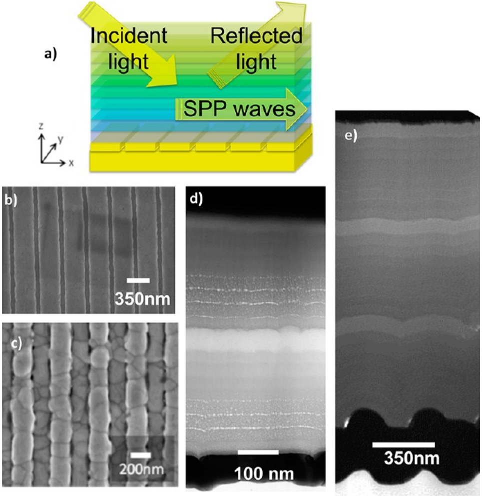

[12] A. Shoji Hall et al., ACS NANO **7**(2013) 4995-5007.

Grating profiles II

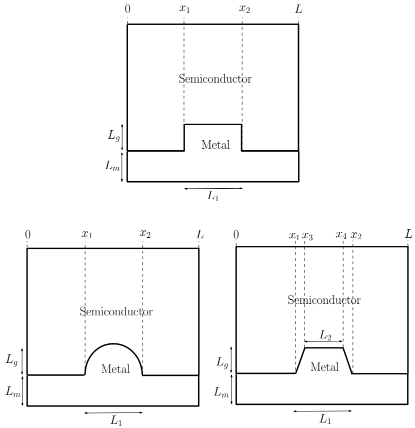

Unit cell of a surface-relief grating with a (top) rectangular corrugation, (bottom left) sinusoidal corrugation, or (bottom right) trapezoidal corrugation.

RCWA validation

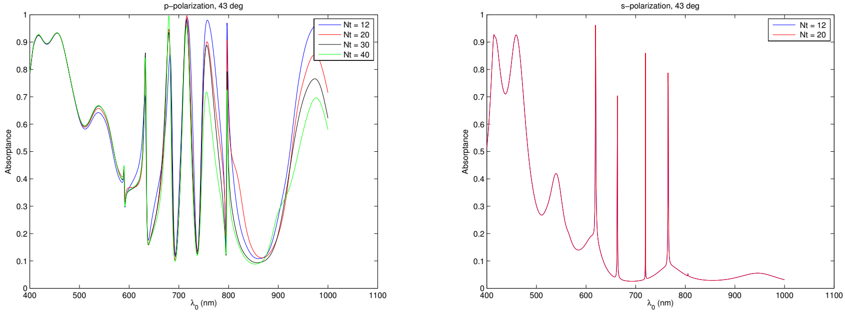

Trapezoidal grating . Duty cycle 0.86. Upper dimension = 251 nm, $\theta = 43°$

FEM Validation

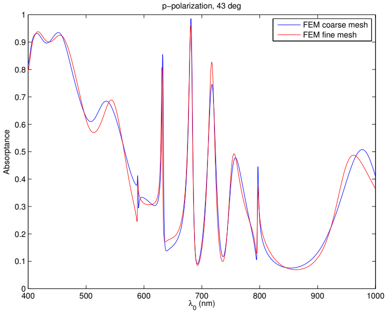

Trapezoidal grating. Duty cycle 0.86. Upper base = 251 nm, $\theta = 43°$. FEM convergence (left)

FEM/RCWA Validation

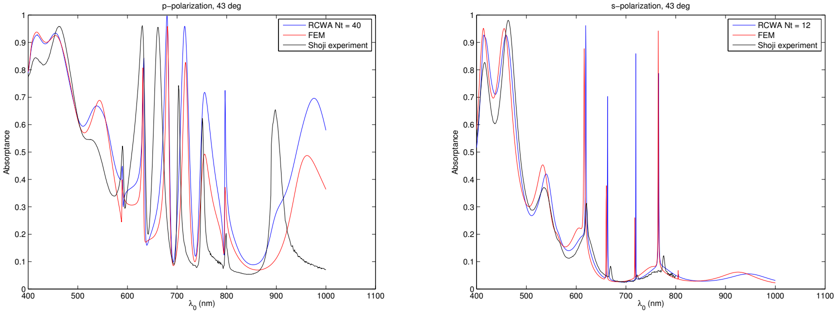

Trapezoidal grating. Duty cycle 0.86. Upper base = 251 nm, $\theta = 43^\circ$, experimental results by Dr. Shoji Hall.

Comparison to experiment: s-polarization

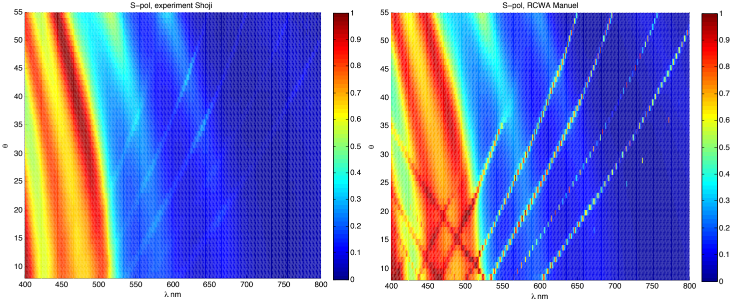

Left panel: experiments by S. Hall. Right Panel: RCWA by M. Solano. Two periods of photonic crystal.

Comparison to experiment: p-polarization

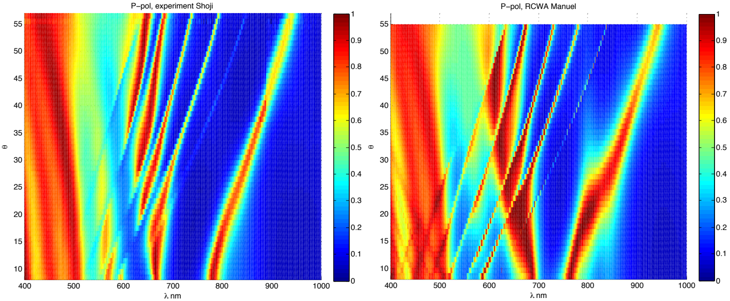

Left panel: experiments by S. Hall. Right Panel: RCWA by M. Solano.

FE Convergence - planar back reflector

Errors and rates of convergence for the FEM when the metallic backreflector is planar and $\theta = 0^\circ$.

ℓ	N_e	e_{Ap}	r_{Ap}	e_{As}	r_{As}
1	342	4.30×10^{-5}	$-$		
2	1880	3.64×10^{-6}	1.15	2.99×10^{-6}	3.13
3	7520	1.97×10^{-7}	4.21	1.91×10^{-7}	3.97
4	30080	1.16×10^{-8}	4.08	1.21×10^{-8}	3.98
5	120320	7.07×10^{-10}	4.04	7.58×10^{-10}	3.99

FE/RCWA convergence for rectangular grating

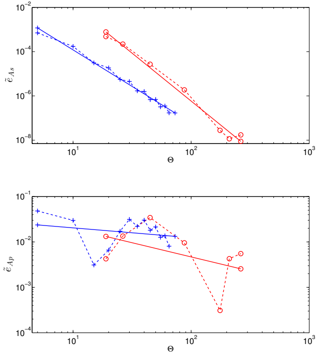

Errors (top) $\tilde{e}_{As}$ and (bottom) $\tilde{e}_{Ap}$ versus Θ calculated with the RCWA ($+$) and FEM ($\circ$) when $\theta = 0^\circ$.
$\Theta = N$ for RCWA, $\Theta = \sqrt{N_{dof}}$ for finite elements (uniform mesh).

Source of the FE error

The solution looses regularity at the metal-dielectric corners. Expect $O(h^{0.06})$ in H^1 norm. [13]

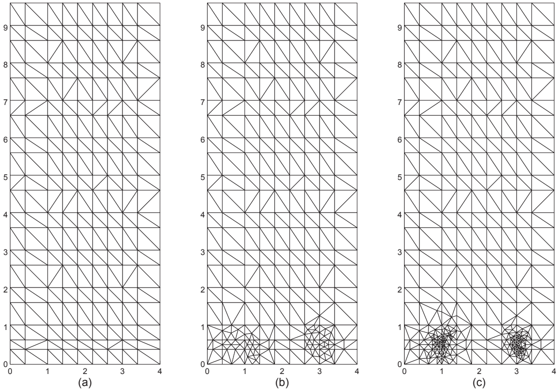

FE solution: refine near the offending point.

[13] J. Elschner and G. Schmidt, *Math. Meth. Appl. Sci.* **21**, 1297-1342 (1998).

Refinement improves reliability

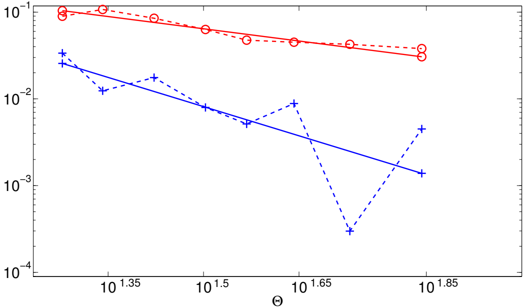

Errors $\tilde{e}_{Ep}$ ($+$) and $\tilde{e}_{Ap}$ ($\circ$) versus Θ calculated with the refined meshes when $\theta = 0^\circ$

Splitter geometry

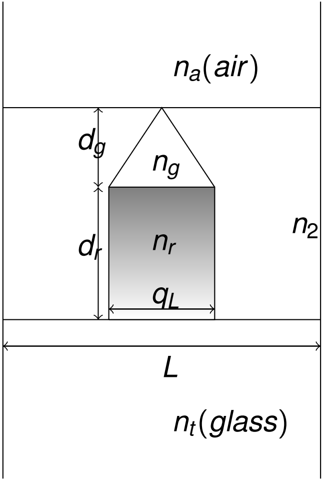

Optimize over L, d_r, d_g, q_L, n_2, n_g (each in a limited range).

Optimization of the Splitter

We want to send waves at frequencies below a cutoff frequency c in the specular direction and waves above that frequency in non-specular directions with no loss due to reflection. We set

$$F = \int_{\lambda_{min}}^{\lambda_{max}} 0.1 \left[(T_{ss}^{0}(\lambda) - H(\lambda - c))^2 + (T_{ss}^{n\neq 0}(\lambda) - (1 - H(\lambda - c)))^2 \right]$$
$$0.9 \left[(T_{pp}^{0}(\lambda) - H(\lambda - c))^2 + (T_{pp}^{n\neq 0}(\lambda) - (1 - H(\lambda - c)))^2 \right] d\lambda$$

where $H(x)$ is the Heaviside step function and $c = 650nm$.

Differential Evolution Algorithm

We use a genetic algorithm called the Differential Evolution Algorithm[14]. Suppose we want to maximize $f(\boldsymbol{v})$. DEA requires three parameters $C \in (0, 1)$ the *crossover probability*, $\alpha \in (0, 2)$ the *differential weight* and M the number of vector initial guesses (we use $C = 0.7$, $\alpha = 0.8$ $M = 10\#parameters$).

The steps to find $\boldsymbol{v}^{opt} \in \mathcal{S}$ are given on the next slide

mutation$\rightarrow$recombination$\rightarrow$selection

[14] Storn, R. and Price, K. (1997), Differential Evolution - A Simple and Efficient Heuristic for Global Optimization over Continuous Spaces, Journal of Global Optimization, 11, pp. 341-359.

DEA

Randomly initialize a set of M vectors: $\{\mathbf{v}^{(m)}\}_{m=1}^{M} \subset \mathcal{S}$

while stopping criterion is not satisfied **do**

  for each $\mathbf{v}^{(\nu)}$, $\nu \in \{1, M\}$, **do**

    Randomly choose three different $\mathbf{v}^{(m_1)}, \mathbf{v}^{(m_2)}, \mathbf{v}^{(m_3)}$

    Choose a random index $j \in \{1, ..., n\}$

    for all $\ell \in \{1, ..., n\}$ **do**

      Pick $r_\ell \in U(0,1)$ to be a uniform random number in (0,1).

      if $r_\ell < C$ or $\ell = j$ **then**

        $w_\ell \leftarrow v_\ell^{(m_1)} + \alpha(v_\ell^{(m_2)} - v_\ell^{(m_3)})$

      else

        $w_\ell \leftarrow v_\ell^{(\nu)}$

      end if

    end for

    if $f(\mathbf{w}) > f(\mathbf{v}^{(\nu)})$ **then**

      $\mathbf{v}^{(\nu)} \leftarrow \mathbf{w}$

    end if

  end for

  $\mathbf{v}^{opt}$ is the vector for which $f(\mathbf{v}^{opt}) \geq f(\mathbf{v}^{(\nu)}) \quad \forall \nu \in \{1, ..., M\}$

end while

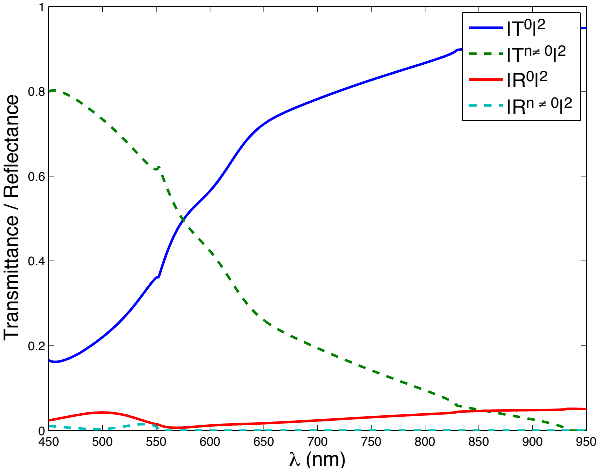

Before the optimization: $L = 500$, $q_L = 250$, $d_t = 300$, $d_r = 100$, $n_t = 1.9$ and the incident angle is 6°.

Differential Evolution optimization starts with:

$$
\begin{aligned}
L &\in [300\ nm, 600\ nm] \\
d_t &\in [50\ nm, 300\ nm] \\
d_r &\in [50\ nm, 300\ nm] \\
n_t &\in [1.1, 1.9] \\
q_L/L &\in [0.1, 0.5]
\end{aligned}
$$

Optimized Results

Optimized Results, $L = 600$, $q_L = 240$, $d_t = 300$, $d_r = 255$, $n_t = 1.9$

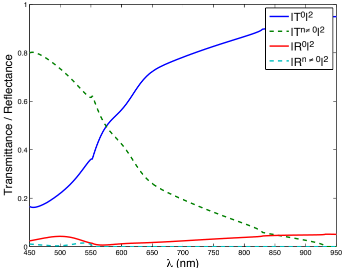

Before

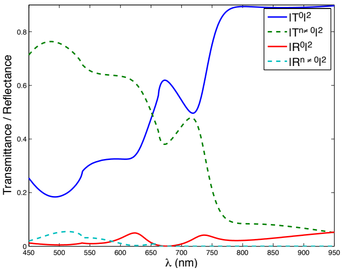

After

Objective function

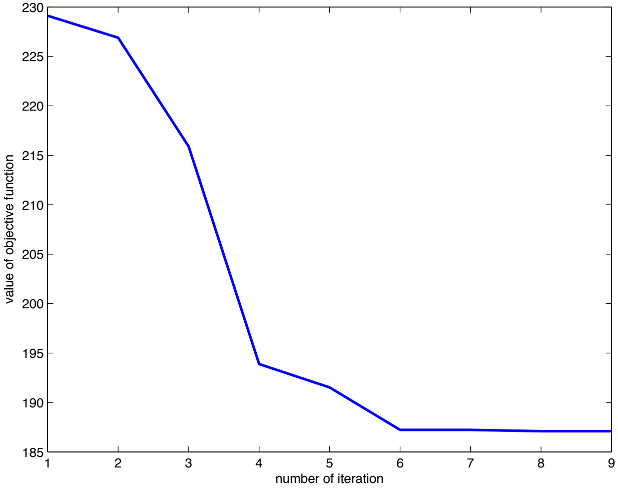

The Time Domain

Let $S = (0, L) \times \mathbb{R}$. Taking the inverse Fourier transform of the s-polarized time harmonic problem (setting n real and ignoring frequency dependence!!) we get that the scattered field $u^s = u^s(x, z, t)$ satisfies

$$
\begin{aligned}
\frac{n}{c^2} u^s_{tt} &= \Delta u^s + \frac{n-1}{c^2} u^i_{tt} \text{ in } S \times \mathbb{R} \\
u^s(\cdot, 0) &= 0 \text{ in } S \\
u^s_t(\cdot, 0) &= 0 \text{ in } S \\
u^s(L, z, t) &= u^s(0, y, t - d_1 L/c) \text{ in } \mathbb{R} \times \mathbb{R}.
\end{aligned}
$$

where $\mathbf{d} = (\sin\theta, \cos\theta)$. We assume that $u^i(x, z, t) = f(t - \mathbf{x} \cdot \mathbf{d}/c)$ where f is such that $f(ct - \mathbf{x} \cdot \mathbf{d}) = 0$ for $t < 0$ and $(x, y) \in [0, L] \times [0, H]$ (e.g. a windowed and translated power of the sine function).

Change of variables

Common to use the change of variables

$$w(x,z,t) = u^s(x,z,t+(x-L)d_1/c)$$

Then recalling $S = ((0,L)\times\mathbb{R})$ we see that

$$\begin{aligned}
\frac{n-d_1^2}{c^2}w_{tt} &= \Delta w - 2\frac{d_1}{c}w_{xt} + \frac{n-1}{c^2}w^i_{tt} \text{ in } S\times\mathbb{R}\\
w(\cdot,0) &= 0 \text{ in } S\\
w_t(\cdot,0) &= 0 \text{ in } S\\
w(L,z,t) &= w(0,z,t) \text{ in } \mathbb{R}\times\mathbb{R}.
\end{aligned}$$

Here $w^i(x,z,t) = f(t-d_2z/c)$.

Analysis in the time domain

Typically implicit methods are used to discretize in time. We can provide an analysis for a small class of methods. To do this we take the Laplace transform

$$\hat{w}(x,z,s) = \int_0^\infty w(x,y,t)\exp(-st)\,dt, \quad s = \sigma - i\omega,$$

where $\sigma \in \mathbb{R}$ is fixed and $\sigma > 0$, while $\omega \in \mathbb{R}$.

Laplace domain problem

Find $\hat{w} \in H^1_p(S)$ such that

$$s^2 \frac{n - d_1^2}{c^2} \hat{w} \;=\; \Delta \hat{w} - 2s \frac{d_1}{c} \hat{w}_x + s^2 \frac{n-1}{c^2} \hat{w}^i \text{ in } (S) \times \mathbb{R}.$$

Here $\hat{w}^i(x, y) = \hat{f}(s) \exp(-sd_1 y/c)$.

The weak Laplace domain problem

For $\hat{w}, \xi \in H^1_p(S)$ define

$$
\begin{aligned}
a(\hat{w}, \xi) &= \int_S \left(\nabla \hat{w} \cdot \nabla \overline{\xi} + s^2 \frac{n - d_1^2}{c^2} \hat{w} \overline{\xi} + 2s \frac{d_1}{c} \hat{w}_x \overline{\xi} \right) \, dA \\
F(\xi) &= s^2 \int_S \frac{n-1}{c^2} \hat{w}^i \overline{\xi} \, dA
\end{aligned}
$$

Then $\hat{w} \in H^1_p(S)$ satisfies

$$
a(\hat{w}, \xi) = F(\xi), \text{ for all } \xi \in H^1_p(S).
$$

Coercivity and continuity

For $\hat{w}, \xi \in H^1_p(S)$ define

$$a(\hat{w}, s\hat{w}) \quad = \quad \int_S \left(\overline{s}|\nabla \hat{w}|^2 + s|s|^2 \frac{n - d_1^2}{c^2} |\hat{w}|^2 + 2|s|^2 \frac{d_1}{c} \hat{w}_x \overline{\hat{w}} \right) \, dA$$

Then

$$\Re a(\hat{w}, s\hat{w}) = \sigma \int_S \left(\overline{s}|\nabla \hat{w}|^2 + |s|^2 \frac{n - d_1^2}{c^2} |\hat{w}|^2 \right) \, dA$$

so provided $n - d_1^2 > \alpha > 0$ for some constant α

$$\Re a(\hat{w}, s\hat{w}) \geq \sigma \min(1, \alpha) \|\hat{w}\|^2$$

where

$$\|\hat{w}\|_1^2 = \int_S \left(|\nabla \hat{w}|^2 + \frac{|s|^2}{c^2} |\hat{w}|^2 \right) \, dA$$

Laplace domain result

Obviously

$$|F(s\hat{w})| \leq C|s|^2 \|\hat{w}^i\|_{L^2} \|\hat{w}\|_1$$

Lemma

Suppose $\alpha > 0$. For each $s = \sigma - i\omega$, $\sigma > 0$, there exists a unique solution $\hat{w} \in H^1_p(S)$ of the Laplace domain problem and

$$\|\hat{w}\|_1 \leq C\frac{|s|^2}{\sigma} \|\hat{w}^i\|_{L^2}$$

Taking the inverse Laplace transform establishes existence of the time domain solution in suitable space-time function spaces (note the exponential weight $\exp(-2\sigma t)$ in the time direction). A good choice might be $\sigma = 1/T$.

Time domain result

Using Lubich's convolution quadrature theory[15] if Backward Euler (p=1) or BDF2 (p=2) are used to discretize the problem (leaving space continuous) at time steps $t_n = n\Delta t$, and if a sufficiently smooth (in time) incident field is used, then

$$\|\nabla(w(\cdot, t_n) - w_n^{\Delta t})\| + \|w(\cdot, t_n) - w_n^{\Delta t}\| = O(\Delta t^p),\ 0 < t < T,$$

where $\Delta t > 0$ is the time step size and $w_n^{\Delta t} \in H_p^1(S)$ is the discrete in time solution at t_n.
We have yet to analyze the spatial discretization.

[15] C. Lubich, *Numer. Math.* **67**, 365-389 (1994).

Current work

- Optimization of the concentrator with matching layers, and other splitter designs.
- 3D grating structure
- Complete analysis of the time domain problem with frequency dependent materials properties.